

# Stark effect and Franz-Keldysh effect of a quantum wire realized by conjugated polymer chains of a diacetylene 3NPh2

Gerhard Weiser

*Fachbereich Physik, Philipps-Universität Marburg, 35032 Marburg, Germany*

Laurent Legrand, Thierry Barisien, Antoine Al Choueiry, and Michel Schott

*Institut des NanoSciences de Paris (INSP), UMR 7588/CNRS, Université Pierre et Marie Curie (Paris 6), Campus Boucicaut, 140 rue de Lourmel, 75015 Paris, France*

Sylvain Dutremez

*Institut Charles Gerhardt Montpellier, UMR 5253/CNRSUM2-ENSCM-UMI, Equipe CMOS, Université Montpellier II, Place Eugène Bataillon, 34095 Montpellier Cedex 5, France*

(Received 22 January 2010; published 22 March 2010)

Conjugated polymer chains diluted in monomer single crystals of a diacetylene, 1,10-bis(diphenylamino)-4,6-decadiyne, represent quantum wires of long-range coherence. They differ from most polydiacetylenes by their repeat unit that consists of two  $C_4$  units with twisted molecular planes. The resulting modification of exciton and band states is studied by electroabsorption which resolves an increase in the exciton transition energy to 2.399 eV and of the free-electron gap to 3.158 eV. The Stark shift of the exciton reveals a significant reduction in the exciton radius by about 40% to  $6 \pm 1$  Å which is consistent with a similar increase in the exciton binding energy to 759 meV. The line shape of electroabsorption spectra at the free-electron gap is for fields larger than 30 kV/cm in accordance with the one-dimensional Franz-Keldysh effect and yields a reduced mass of  $0.07m_0$  larger than in other polydiacetylene (PDA). Spectra at smaller fields are distorted by contributions of a weak dipole allowed and a forbidden exciton 38 and 12 meV, respectively, below the band gap. Coherent coupling of free electrons and vibrational modes leads to replicas of the Franz-Keldysh effect. Since light polarized parallel to the conjugated chain excites two propagating modes in the monomer crystals the quantitative analysis was restricted to electroabsorption spectra taken with perpendicular polarization in samples which transmit only the weakly absorbed polariton mode.

DOI: [10.1103/PhysRevB.81.125209](https://doi.org/10.1103/PhysRevB.81.125209)

PACS number(s): 78.40.Me, 71.35.Cc, 71.70.Ej, 78.20.Jq

## I. INTRODUCTION

Polydiacetylenes (PDAs) are still unique among conjugated polymers since they can be prepared through solid-state polymerization in a highly ordered state.<sup>1</sup> Large side-groups attached to the diacetylene molecule reduce interchain interaction while  $\pi$ -conjugation delocalizes the corresponding electron states. As criteria were developed for successful polymerization in monomer single crystals<sup>2-7</sup> two classes of PDAs emerged with a strong fundamental exciton centered either near 2.0 or 2.3 eV which are called blue and red chains by the color of partially polymerized crystals. Despite that difference x-ray and Raman studies indicate the same basic building block,  $-C \equiv C - C = C-$ . Long-range coherence within the polymer chains enables in some cases the detailed study of their electronic structure by electroabsorption spectroscopy as in wide band semiconductors. The free-electron gap is resolved by a pronounced Franz-Keldysh effect although its absorption is hidden under vibronic progressions of a strong exciton which responds to an external field by a quadratic Stark shift.<sup>8</sup> The electroabsorption (EA) spectra yield not only the band gap and an exciton binding energy of about 500 meV but derive from field broadening of Franz-Keldysh oscillations a reduced mass of about  $0.05m_0$  of blue chains in DCH [1,6-di(N-carbazolyl)-2,4-hexadiyne] polymer single crystals<sup>9</sup> and those diluted in monomer single crystals of 3BCMU and 4BCMU,<sup>10</sup> much smaller than the free-electron mass  $m_0$ .

Controlled polymerization in single crystals provides  $\pi$ -conjugated chains with properties expected for quantum wires of very small radius and luminescence studies on red chains of 3BCMU proved the one-dimensional density of states of the exciton band.<sup>11,12</sup> Coherent coupling of excitons on a single chain to a propagating laser field was verified by microfluorescence<sup>13</sup> and by spatially coherent emission of a single chain.<sup>14,15</sup> By increasing the density of blue chains coherent coupling of excitons to radiation modes of the monomer crystal leads to a tightly bound polariton which enables transmission of light in resonance to the exciton through thick crystals of 3BCMU.<sup>16,17</sup> Despite such unique properties the very same  $C_4$  building block leaves little room for variation in these quantum wires. A promising modification is doubling the repeat unit as in poly-THD [1,6-bis(diphenylamino)-2,4-hexadiyne] where  $C_4$  units are alternatively tilted by  $\pm 7.5^\circ$  relative to their average plane.<sup>18-20</sup> The large thermal reactivity of this monomer prevented studies of highly diluted chains but electroreflectance spectra of opaque crystals resolved the exciton at 2.171 eV and the band gap at 2.727 eV.<sup>19</sup> Although the exciton transition energy is larger than that of blue chains the binding energy 0.56 eV is similar and lends no support to a significant change in the electronic structure.

Synthesis of several analogues of THD led to 3NPh2 [1,10-bis(diphenylamino)-4,6-decadiyne] as material of proper reactivity for controlled polymerization. Two pairs of

TABLE I. Crystal parameter of 3NPh2 at 180 K (Ref. 21).

$a$ (Å)	$b$ (Å)	$c$ (Å)	$\beta$
9.9484	16.0893	16.7643	98.697°
$Z=4$ , $V=2652.5 \text{ \AA}^3$ , $M=468.62 \text{ g mol}^{-1}$			

molecules with twisted molecular planes stack along the  $a$ -axis of the monomer crystal and polymerization proceeds along that axis. The inequivalent molecules in the host crystal double the polymer repeat unit and calculations indicate substantial tilting of the  $C_4$  units by  $\pm 20^\circ$ .<sup>20,21</sup> Absorption and luminescence spectra submitted in context with the present paper show a remarkable increase in the exciton transition energy to 2.4 eV, larger than in any other PDA.<sup>22</sup> We present here supplementary electroabsorption spectra which despite unexpected birefringence effects confirm not only the anticipated change in the electronic structure but show an excellent agreement of the spectra at the band gap with the Franz-Keldysh effect of a one-dimensional energy band.

## II. EXPERIMENTAL DETAILS

The molecules crystallize in the monoclinic space group  $P21/n$  with  $Z=4$  (Table I) and pile up along the  $a$  axis with alternating stacking distance of 4.917 Å and 5.329 Å. The lattice constant  $a=9.948$  Å is slightly larger than twice the usual  $C_4$  repeat unit of relaxed PDA chains. Details of the structure and polymerization of 3NPh2 are given elsewhere.<sup>21,22</sup>

Crystals were grown in the dark from a solution in acetone at 4 °C reaching about 5 mm length along the  $a$  axis and their thickness (0.2–0.4 mm) was measured by focusing a microscope on the front and back surface. The small initial polymer content was increased by  $\gamma$ -irradiation from a  $^{137}\text{Cs}$  source with a dose of 5 krad/min. Cr/Al contacts were evaporated onto the 0.5–0.7 mm broad (010) face, which as largest face was chosen to apply a sinusoidal field of 1 kHz frequency along the polymer backbone. Light from a tungsten halide lamp or a xenon arc was dispersed by a single-pass monochromator with bandpass of 4 and 2 Å, respectively, polarized by a calcite polarizer and focused onto the sample which was mounted onto the cold finger of a He cryostat. The transmitted light was collected by a photomultiplier and its intensity measured by a voltmeter. The modulated part  $\Delta I$  was analyzed by a lock-in amplifier tuned to twice the frequency of the applied field. The ratio of peak voltage and electrode gap of 0.5 mm defines the field strength and the change  $\Delta\alpha$  of the absorption constant was derived from the ratio of the relative change in transmitted light intensity and thickness  $d$  of the sample.

$$\Delta\alpha = -\frac{1}{d} \frac{\Delta I}{I}. \quad (1)$$

Since the lock-in amplifier returns the effective value of the selected Fourier component the reading has been scaled to the amplitude of  $\Delta I$  by an appropriate factor which is  $2\sqrt{2}$  in

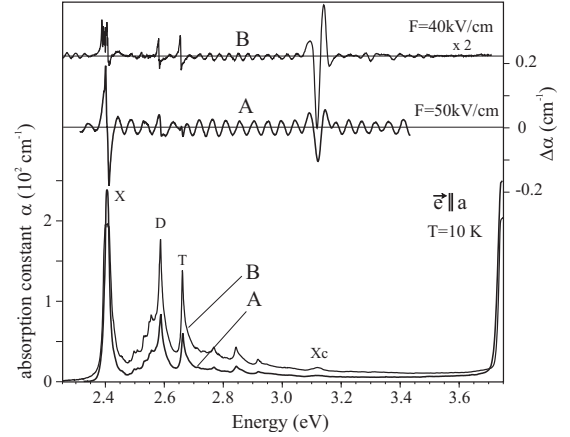


FIG. 1. Absorption and electroabsorption spectra with light polarized parallel to the conjugated chains in samples A and B exposed for 1 and 3 min to  $\gamma$  radiation. The EA spectrum of sample B is enlarged as indicated to fit into the scale.

case of a quadratic response to a sinusoidal field.

## III. EXPERIMENTAL RESULTS

### A. Samples with low polymer content

#### 1. Absorption and electroabsorption spectra

Transmission studies with light polarized parallel to the conjugated chain,  $\vec{e} \parallel a$ , require samples with low polymer concentration. Figure 1 compares spectra of samples A and B exposed to  $\gamma$ -radiation for 1 and 3 min, respectively. All features below the monomer absorption threshold at 3.7 eV belong to  $\pi-\pi^*$  transitions of conjugated chains. The absorption spectra show an exciton peak X at 2.4 eV with strong satellites D and T due to coupling to stretch modes of double and triple bond. These features are typical for polydiacetylene and the narrow linewidth confirms an excellent quality of the samples. Combination modes lead to more peaks at higher energy and additional vibronic excitons appear about 100 meV above the exciton. The spectra show also a small peak Xc at 3.12 eV which does not fit into a vibronic progression. The apparently smaller exciton peak in sample B is an artifact caused by its larger thickness. The corresponding transmittance is about 1% for the 190  $\mu\text{m}$  thick sample A but only 0.07% for the 360- $\mu\text{m}$ -thick sample B which is not much above the background of scattered light.

The upper traces in Fig. 1 display the electroabsorption spectra. The exciton of sample A responds by a quadratic Stark shift which leads to the derivativelike shape of  $\Delta\alpha$ . Another strong signal of different line shape and weaker field strength dependence appears at 3.1 eV. Similar signals far above the exciton in other PDA have been attributed to the Franz-Keldysh effect at the free-electron gap.<sup>8</sup> A new feature is the regular pattern with 46.2 meV period and almost constant amplitude which is distorted only by the response of the strong vibronic excitons. Sample B with larger polymer concentration shows a similar pattern of 32.6 meV period but smaller amplitude which allows resolving the response of the vibronic excitons D and T. The noisy spectrum at 2.4 eV

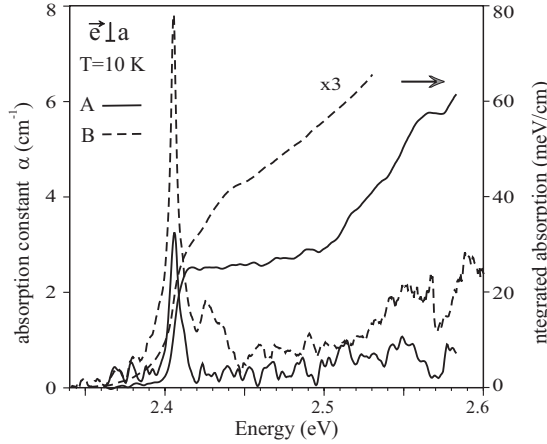


FIG. 2. Absorption and integrated absorption for polarization of light perpendicular to the chain.

shows some splitting of the exciton which is also observed in sample A. The most prominent feature occurs again far above the exciton with the strong negative peak at the same energy as the weak absorption peak Xc at 3.12 eV.

Absorption spectra for light polarized perpendicular to the chain are presented in Fig. 2 together with the integrated absorption. The exciton peak of sample A is with  $3 \text{ cm}^{-1}$  about 100 times smaller than for polarization parallel to the chain and has smaller linewidth.<sup>22</sup> We therefore use the integrated absorption,  $S=5.2$  and  $0.027 \text{ eV/cm}$  for polarizations parallel and perpendicular to the chain, respectively, to derive an optical anisotropy close to 200. The sum rule of the oscillator strength  $f$  provides also an estimate of the polymer content  $x_p$ ;

$$f = \frac{4\pi c^2 \epsilon_0 n}{h c e^2 N} \int_{\text{peak}} \alpha(E) dE = x_p \times f_{PDA}, \quad (2)$$

where  $N=1.5 \times 10^{21} \text{ cm}^{-3}$  is the density of diacetylene molecules. With  $n=1.5$  as refractive index of the host crystal and the typical oscillator strength  $f_{PDA}=0.5$  of the exciton the fraction of polymerized diacetylene molecules in sample A is  $x_p=6 \times 10^{-5}$ . Since the exciton peak of sample B is obviously truncated we derive the polymer content  $x_p=13.2 \times 10^{-5}$  from the peak height of the vibronic satellites D and T which exceeds those in sample A by a factor of 2.2. These concentrations yield a polymerization rate  $dx_p/dt=3.6 \times 10^{-5}/\text{min}$  which corresponds to a rate of  $0.72\%/ \text{Mrad}$  in satisfactory agreement with the rate  $0.75\%/ \text{Mrad}$  obtained from the weight of insoluble material of  $\gamma$ -irradiated crystals.<sup>21</sup>

## 2. Optical birefringence

The periodic pattern of the EA spectra and the saturated optical density of the exciton for light polarized along the chain in samples of higher polymer content results from optical birefringence of the monoclinic crystal. The saturation cannot result from undamped propagation of a tightly bound polariton state of exciton and photon as in 3BCMU since it is independent of temperature.<sup>16</sup> Light of polarization  $\vec{e} \parallel a$  provides best coupling to the transition dipoles of the chain but

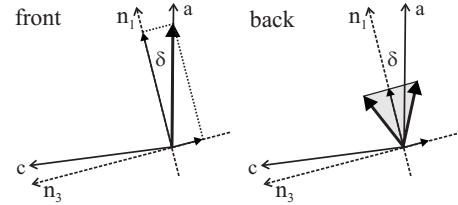


FIG. 3. Polarization of propagating modes excited by light polarized parallel to the  $a$  axis on the  $ac$  face of a monoclinic crystal. Different attenuation and phase rotate the polarization of transmitted light within the shaded cone.

excites on the  $ac$  face two propagating electromagnetic waves of orthogonal polarization since only the  $b$ -axis defines a principal axis of the dielectric tensor.<sup>23</sup> The other axes lie in the  $ac$  plane and electric fields polarized along these axes propagate with refractive indices  $n_1$  and  $n_3$ . If the axis  $n_1$  is rotated by  $\delta$  out of the  $a$  axis the orthogonal mode with refractive index  $n_3$  acquires the fraction  $\sin^2 \delta$  of light with polarization  $\vec{e} \parallel a$  (Fig. 3). Measurements with crossed polarizers indicate a rotation by  $\delta=2.5^\circ \pm 1^\circ$  which couples 0.2% of light of polarization  $\vec{e} \parallel a$  into the weakly absorbed mode. Since light polarized perpendicular to the chain,  $\vec{e} \perp a$ , excites also the strongly absorbed mode its absorption is enhanced which reduces the optical anisotropy further. The true anisotropy of the exciton therefore is obscured by the birefringence of the crystal since the exciton dipole  $\vec{\mu} \parallel a$  is a source for the electric field of either propagating wave.

When the waves arrive at the back of the sample their fields add up to the polarization  $\vec{e}$  of transmitted light. This polarization deviates from  $\vec{e} \parallel a$  at the front surface due to different loss and the phase difference  $\phi$  accumulated along the optical path of length  $d$ :

$$\vec{e} = \exp(in_1 kd - i\omega t) [\vec{e}_1 + \vec{e}_2 \exp(i\phi)],$$

$$\phi = (n_3 - n_1) kd = (n_3 - n_1) \frac{\omega}{c} d. \quad (3)$$

The transmitted light is linearly polarized in the  $ac$  plane and the field vector rotates according to the phase difference within a cone defined by  $\phi$  being an even or odd multiple of  $\pi$  which opens up with decreasing amplitude of the strongly absorbed mode. Since the fields of the propagating modes are orthogonal the phase has no effect on the transmitted light intensity which,  $c$  and  $\epsilon_0$  denoting the speed of light and vacuum permittivity, is the sum of the intensities of both modes.

$$I = c \epsilon_0 \vec{e} \cdot \vec{e}^* = c \epsilon_0 \{ |\vec{e}_1|^2 + |\vec{e}_2|^2 + 2\vec{e}_1 \cdot \vec{e}_2 \cos \phi \}. \quad (4)$$

The phase is important if the polarization  $\vec{P} = \epsilon_0 \chi \vec{e}$  as part of a propagating wave couples to the modulation field  $\vec{F}$ . The tensor  $\chi$  of the optical susceptibility rotates the polarization with respect to the driving fields  $\vec{e}_1$  and  $\vec{e}_2$  and the field-induced change  $\Delta \vec{P}$  of the polarization, given by the coupling strength  $\vec{P} \cdot \vec{F}$ , accumulates along the optical path. The emitted field-modulated intensity  $\Delta I$  is described by tensor components  $S_j$  of a nonlinear susceptibility which depend on

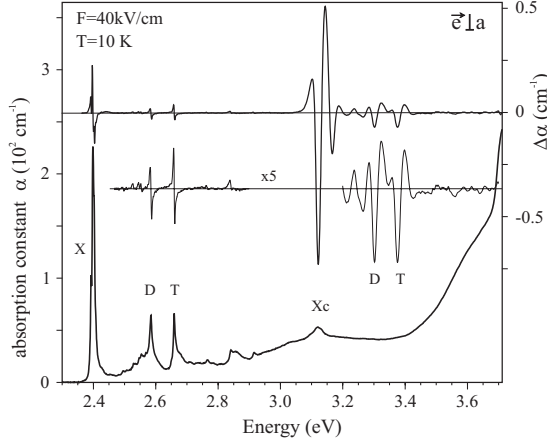


FIG. 4. Absorption and electroabsorption spectra of sample C exposed for 2 h to  $\gamma$  radiation. Part of the EA spectrum is enlarged by the factor of five to resolve the vibronic replicas of the strong features. Polymer concentration  $\eta \approx 0.5\%$ .

products of the polarization  $\vec{e}$  of the propagating waves and the applied field  $\vec{F}$ ;

$$\Delta I = S_1 |\vec{e}_1 \cdot \vec{F}|^2 + S_2 |\vec{e}_3 \cdot \vec{F}|^2 + 2S_3 (\vec{e}_1 \cdot \vec{F})(\vec{e}_3 \cdot \vec{F}) \cos \phi. \quad (5)$$

Two terms in Eq. (5) are proportional to the intensity of the modes but the third term depends on their phase difference  $\phi$ . The phase increases with the frequency of light and maxima appear in the modulated transmittance when the phase difference is a multiple of  $2\pi$ . Negligible dispersion of the refractive indices below the absorption edge of the monomer leads in samples of small polymer concentration to a periodic pattern of  $\Delta I$  with the period given by the difference of the refractive indices and the crystal thickness  $d$ :

$$(n_3 - n_1) \frac{\omega_j}{c} d = j \times 2\pi \Rightarrow \Delta \hbar \omega = \frac{hc}{(n_1 - n_3)d}. \quad (6)$$

The periodicity 46.2 meV for the 190- $\mu\text{m}$ -thick sample A and 32.6 meV in for 360- $\mu\text{m}$ -thick sample B yields similar values  $|n_3 - n_1| = 0.14$  and 0.11, respectively, which depend sensitively on the sample thickness. The periodic signal thus results from the optical Kerr effect, the field-induced change in refractive indices, and the almost constant amplitude indicates that it is mainly a response of the host crystal.

TABLE II. Transition energies of the exciton X and some vibronic satellites and of the peak Xc in sample C with 0.5% polymer concentration.

Transition	X	$\nu_1$	$\nu_2$	$\nu_3$	D	T	Xc
Energy (eV)	2.4025	2.4956	2.5070	2.5293	2.5846	2.6595	3.120
Difference to X (meV)		93.1	104.5	126.8	182.1	257.0	718

## B. Samples with large polymer content

### 1. Survey of absorption and electroabsorption spectra

The periodic pattern due to optical birefringence vanishes if one mode is completely absorbed. Consequently, better field-modulated spectra are expected from samples of larger polymer content and with polarization  $\vec{e} \perp a$ . Figure 4 displays absorption and electroabsorption spectra of the 200- $\mu\text{m}$ -thick sample C exposed for 2 h to  $\gamma$ -irradiation with polymer fraction  $x_p = 0.46\%$ . It is emphasized that neither the concentration nor the thickness of the sample enter into the evaluation of the field response of the chain.

The absorption spectrum reproduces all features observed with polarization  $\vec{e} \parallel a$ . It shows an absorption background which increases towards higher energy and may result from light scattering by polymer chains. The periodic pattern of  $\Delta \alpha$  has vanished as expected and the EA spectrum resolves many sharp structures and the largest signal occurs above 3.1 eV at the position of the absorption peak Xc. All features at lower energy increase quadratically with the field strength and without change in their line shape in agreement with the quadratic Stark effect. The strong signal above 3.1 eV has weaker dependence on the field and shows field broadening as expected for the Franz-Keldysh effect in the high-field regime.

Table II presents the transition energies of the exciton X, with some of its weak satellites  $\nu_j$  and strong satellites D and T and of the absorption peak Xc. The exciton splits into several narrow lines separated by a few meV and the vibronic energies are taken from the distance of the respective peaks to the main exciton line. With the high-energy signal attributed to the free-electron gap the exciton binding energy exceeds 700 meV and the absorption peak Xc could arise from the singularity of the density of states at the gap of a one-dimensional band.

Absorption spectra of this sample with polarization  $\vec{e} \parallel a$  are shown in Fig. 5. The flat absorption above 2.4 eV corresponds to the total loss of the strongly absorbed mode. The residual transmittance (0.4%) is due to the simultaneously excited weakly absorbed mode which by its absorption generates the small features on top of the saturation level. Additional states are observed below 2.4 eV and the derivative lineshape of their EA spectrum is attributed to the Stark shift of excitons with transition energies of 2.2475, 2.2815, and 2.3798 eV. Similar field-sensitive excitons of unknown origin have been observed in 3BCMU and 4BCMU.<sup>10</sup> The spectrum at room temperature shows again the thermal broadening and blue shift of the absorption edge.

### 2. Temperature and field-strength dependence

The thermal broadening of the exciton and blue shift is shown elsewhere<sup>22</sup> and appears also in the electroabsorption

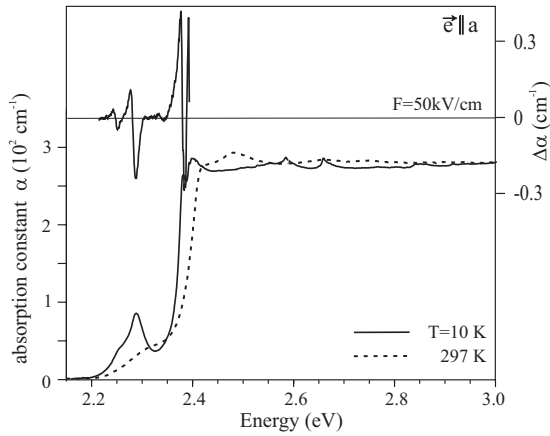


FIG. 5. Absorption and electroabsorption spectra for polarization parallel to the chain in sample C with 0.5% polymer content.

spectrum. Figure 6 presents spectra above 3.1 eV for several temperatures. They shift with increasing temperature to higher energy at a rate which agrees with the shift of the exciton and thermal broadening decreases the signal until at 297 K only the most prominent peaks survive. It is mentioned that thermal broadening of this spectrum obtained with a large field increases much less than the width of the excitonic features in absorption and electroabsorption spectra.<sup>24</sup>

Field broadening of the EA spectrum above 3.1 eV is demonstrated in Fig. 7. Although expected for the Franz-Keldysh effect<sup>25</sup> it has been observed at similar fields only in semiconductors with small reduced mass such as Ge,<sup>26</sup> GaAs,<sup>27</sup> and InGaAs (Ref. 28) but also in fully polymerized DCH (Ref. 9) and on blue chains in 3BCMU and 4BCMU monomer single crystals.<sup>10</sup> Field broadening leads to a redshift of the first peak at 3.10 eV and a blueshift of all peaks above 3.15 eV. The very small shift of the dominant negative peak at 3.12 eV is consistent with the Franz-Keldysh effect. However, the distorted lineshape at very small fields and the fairly stable position of the strong positive peak near 3.145 eV suggests that additional effects contribute to the EA spectrum.

The series of additional peaks of the EA spectrum at higher energy is shown in Fig. 8 which by their distance

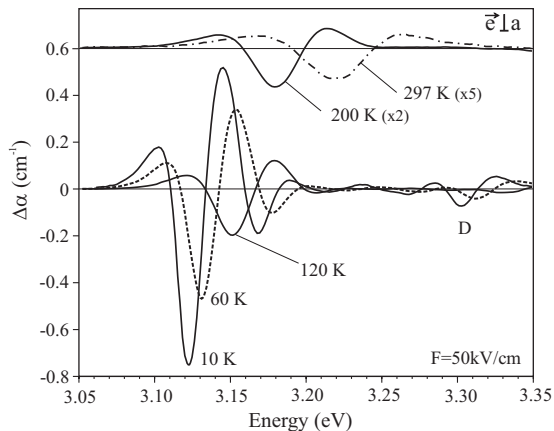


FIG. 6. Temperature dependence of the EA spectrum above 3.1 eV.

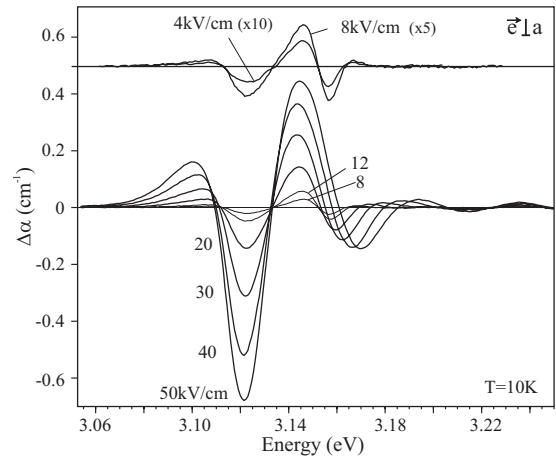


FIG. 7. Variation with field strength of the EA spectrum near 3.12 eV. Spectra at high temperature on top are enlarged as indicated.

from the negative peak at 3.12 eV are attributed to vibronic replicas of the Franz-Keldysh effect of the fundamental gap. The strongest satellites near 3.30 and 3.37 eV show also some field-broadening. The peak at 3.20 eV which shifts with the field belongs to the Franz-Keldysh effect of the gap but not the negative peaks at 3.215 and 3.265 eV which keep their position.

#### IV. EVALUATION OF THE ELECTROABSORPTION SPECTRA

##### A. Stark effect of the exciton

Inversion symmetry of 3NPh2 leads to dipole selection rules of the  $\pi$  electrons based on the parity of states. The field  $F$  couples the dipole allowed exciton  $X$  to states of even parity and energy  $E_j$  which by second-order perturbation theory leads to the quadratic Stark shift;

$$\Delta E_X = \sum_j \frac{|\vec{\mu}_j \cdot \vec{F}|^2}{E_X - E_j}. \quad (7)$$

The energy denominators determine the sign of the contributions and reduce coupling to distant states  $|j\rangle$ . One dipole

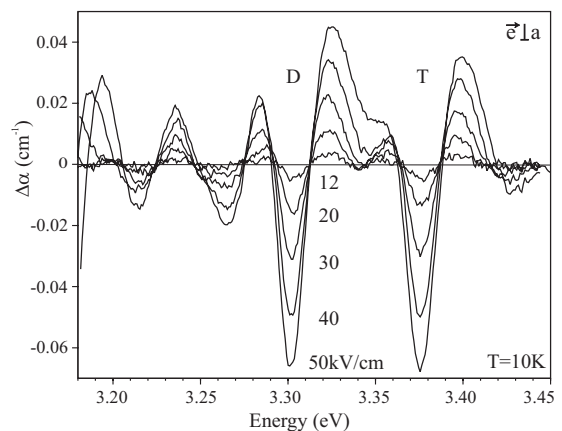


FIG. 8. Field strength dependence of the EA spectrum in the range of vibronic band gaps.

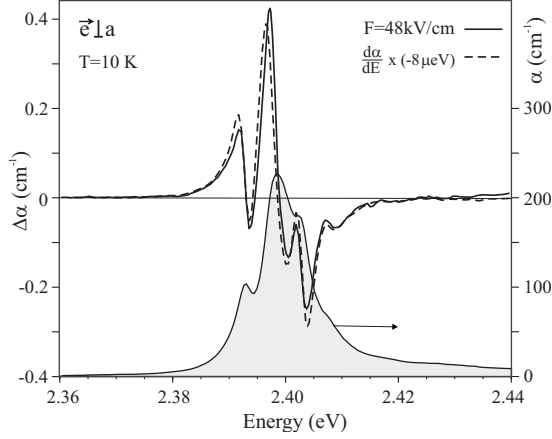


FIG. 9. Comparison of the EA spectrum and the derivative of the exciton absorption (shaded area) scaled to a redshift by 8  $\mu\text{eV}$ .

moment  $\mu_j$  often dominates and for Wannier-type excitons which couple primarily to the free-electron gap at  $E_C$  the corresponding transition dipole is given by the exciton radius,  $e\vec{r}$ , which simplifies its Stark shift;

$$\Delta E_X = \frac{|e\vec{r} \cdot \vec{F}|^2}{E_X - E_C}. \quad (8)$$

By coupling to states of even parity the exciton loses oscillator strength  $\Delta f$  and this loss involves the same transition dipoles as the Stark shift but depends quadratically on the energy denominators;

$$\frac{\Delta f}{f} = - \sum_j \frac{|\vec{\mu}_j \cdot \vec{F}|^2}{(E_X - E_j)^2}. \quad (9)$$

In case of large binding energy,  $(E_X - E_C) \gg \Delta E_X$ , the redshift dominates and the excitonic electroabsorption spectrum is proportional to the derivative of the absorption.

Figure 9 presents the exciton absorption peak with its fine structure that can be fitted to four narrow Lorentzians at 2.3926, 2.3985, 2.4024, and 2.4075 eV. The EA spectrum at 48 kV/cm on top is reproduced by the derivative of the absorption band with a redshift by 8  $\mu\text{eV}$ . Similar agreement is found with the sum of derivatives of the Lorentzians. The common shift of all transitions proves that the four states are not mixed by the electric field but belong to different chains or chain segments.

The same Stark shift is observed for the vibronic satellites D and T at 2.5885 and at 2.6591 eV and even for the weaker satellites as shown in Fig. 10. Consequently, all these features result from coupling the same exciton to forbidden states at higher energy or to the continuum of ionized electron-hole pairs. The first EA signal which is not part of the exciton occurs at 3.12 eV. Line shape and field strength dependence exclude the quadratic Stark effect as origin but agree with the signal of a free-electron band gap. With the energy separation by 0.72 eV and field of 48 kV/cm inserted into Eq. (8) the redshift by 8  $\mu\text{eV}$  yields an exciton radius of 5.0  $\text{\AA}$ . Scaling to the derivative of a narrow absorption spectrum depends on the spectral resolution and the shift is likely

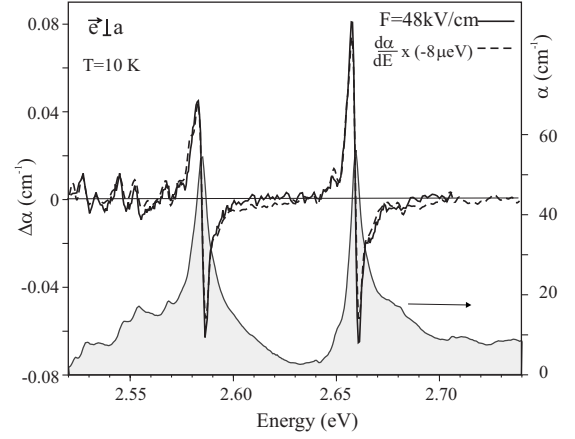


FIG. 10. Comparison of the EA spectrum and the derivative of the absorption of the strong vibronic excitons D and T.

to be larger since the absorption has been measured with narrower bandpass. The Stark shift by 6 and 8  $\mu\text{eV}$  in a field of 36 kV/cm derived from the broadened spectra at 100 K and at room temperature yield an exciton radius of 5.8 and 6.7  $\text{\AA}$ , respectively. The EA spectrum in fig. 1 taken with 50 kV/cm and polarization  $\vec{e}||a$  matches a redshift by 14  $\mu\text{eV}$  which corresponds to an exciton radius of 6.4  $\text{\AA}$ . We conjecture that the exciton radius in poly-3NPh2 is  $(6 \pm 1) \text{\AA}$  which is about 40% smaller than the average value of 10  $\text{\AA}$  found in other PDAs.<sup>8,10</sup> This significant change in the exciton radius is supported by a similar increase in the exciton binding energy from about 0.5 to 0.72 eV.

## B. Franz-Keldysh effect of the band gap

### 1. Franz-Keldysh effect a one-dimensional band gap

The Franz-Keldysh effect describes the optical interband polarization in presence of an electric field. The plane wave envelope of Bloch states in a periodic potential is replaced by the Airy function  $Ai(z)$  as eigenstate of a free electron in a constant electric field.<sup>25</sup> The energy  $W = eFr$  which electrons gain by moving in the field is eliminated by rescaling the kinetic energy  $E - E_g$  of an electron-hole pair to an energy  $\hbar\theta$  which depends on the reduced mass  $\mu$  and on the field;

$$\hbar\theta = \left( \frac{e^2 \hbar^2 F^2}{2\mu} \right)^{1/3}. \quad (10)$$

Scaling to a field-dependent energy leads to field-broadening of the modulated spectra with the peculiar dependence on  $F^{2/3}$ . Lifetime broadening by  $\Gamma$  which limits the range of coherent motion enters as imaginary part of the renormalized energy  $z$  (Ref. 29)

$$z = \xi + i\eta = \frac{E_g - E}{\hbar\theta} + i \frac{\Gamma}{\hbar\theta} \quad (11)$$

and results in the field-induced absorption  $\Delta\alpha$  of a one-dimensional continuum that is described by:<sup>30,31</sup>

$$\Delta\alpha(E) = \frac{B}{2n\omega\sqrt{\hbar\theta}} \left\{ \left[ 2\pi \exp \frac{i\pi}{3} Ai(z) Ai(w) \right] - \frac{\mathcal{H}(-z)}{\sqrt{-z}} \right\},$$

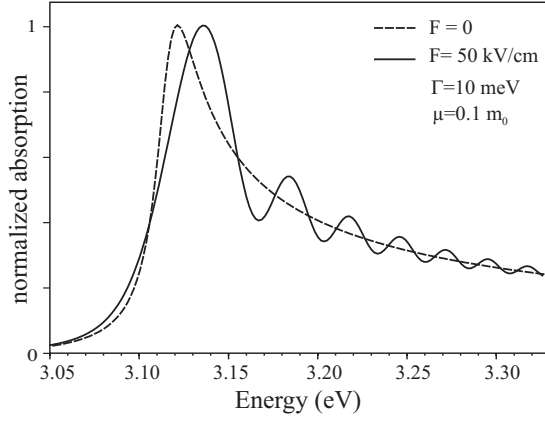


FIG. 11. Absorption spectra of a one-dimensional band with and without an electric field.

$$w = z \exp\left(\frac{-2\pi i}{3}\right), \quad B = \frac{\sqrt{2\mu}e^2}{\epsilon_0 m^2 \omega^2 \hbar} |P|^2. \quad (12)$$

The field-independent part  $B$  of the amplitude accounts for the interband momentum matrix element  $P$  and the refractive index  $n$  enters when the imaginary part of the dielectric response function is replaced by the absorption constant  $\alpha$ . The unity step function  $\mathcal{H}$  represents the field-free case with the  $1/\sqrt{E-E_g}$  singularity of the density of states. The field generates an exponential absorption tail below the gap and oscillations at higher energy extend over the range of energy gained by coherent acceleration. A corresponding expression for isotropic matter describes the electroabsorption spectrum of a cubic semiconductors over more than 0.4 eV.<sup>32</sup>

Figure 11 compares calculated absorption spectra with and without field of one-dimensional bands with small reduced mass and a gap at 3.12 eV. Field and mass correspond to  $\hbar\theta=21.2$  meV and define the argument of the Airy functions which were taken from the Handbook of Mathematical Functions.<sup>33</sup> The broadening parameter  $\Gamma=10$  meV softens the singularity at the gap and the field-free absorption resembles an asymmetric absorption peak. The field shifts the absorption peak to higher energy and the subsequent oscillations reflect the redistribution of the interband polarization. The difference to the field-free absorption predicts an electroabsorption spectrum  $\Delta\alpha$  with a large negative peak at  $E_g$  which is followed by a strong positive peak and weaker oscillations. These oscillations vanish rapidly as  $\hbar\theta$  gets smaller than the broadening parameter  $\Gamma$ . Changes below the

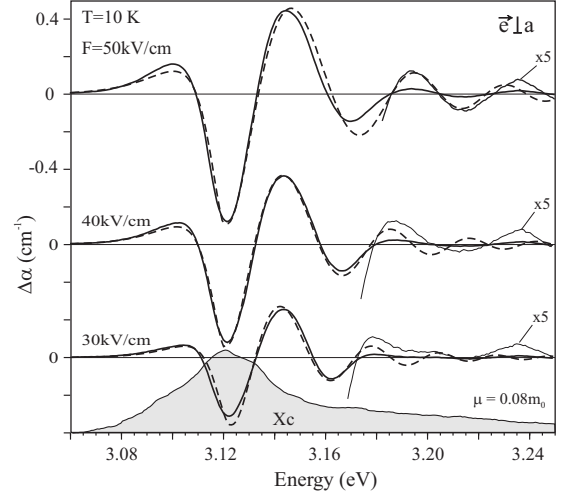


FIG. 12. EA spectra (full lines) for large fields compared with spectra of a one-dimensional Franz-Keldysh effect (dashed lines):  $\Gamma=10$  meV,  $\mu=0.08m_0$ . Weak signals at higher energy are enlarged by a factor of five. The shaded area shows the absorption peak Xc with the background subtracted.

gap are small and generate a broad and rather weak positive peak of  $\Delta\alpha$ . EA spectra with the peculiar dependence on  $F^{2/3}$  were observed for blue chains of polydiacetylene and yield the reduced mass  $\mu \approx 0.05m_0$ . However, all these spectra show a strong positive  $\Delta\alpha$  peak below the gap of similar size as the negative peak at  $E_g$  which does not comply with the predicted lineshape of the Franz-Keldysh effect at a one-dimensional band gap.<sup>9,10</sup>

## 2. Spectra at large electric fields

The one-dimensional Franz-Keldysh effect reproduces the EA spectrum of poly-3NPh2 almost perfectly for large fields as shown in Fig. 12. The broadening parameter  $\Gamma=10$  meV was chosen to match the width of the leading peaks and mass, amplitude and energy gap are listed in Table III. The gap occurs at 3.12 eV at the energy of the weak absorption peak Xc which supports its assignment to the density of states of one-dimensional band gap. The Franz-Keldysh effect reproduces also the small positive peak of  $\Delta\alpha$  below the gap and the position of all oscillations up to 3.22 eV. Peaks above 3.16 eV are smaller than predicted but faster damping with increasing carrier velocity has been observed in semiconductors<sup>32</sup> and is anticipated if the energy of an

TABLE III. Parameters used to fit the one-dimensional Franz-Keldysh effect to the electroabsorption spectrum above 3.1 eV: the energy gap  $E_g$ , the electro-optic energy  $\hbar\theta$  with the corresponding reduced mass  $\mu$ . The normalized amplitude represents the field-independent part.

$F$ (kV/cm)	50	40	30	20	12	8	4
$E_g$ (eV)	3.120	3.120	3.122	3.122	3.122	3.158	3.158
$\hbar\theta$ (meV)	22.83	19.68	16.24	12.96	9.22	7.04	4.43
$\mu$ ( $m_0$ )	0.08	0.08	0.08	0.07	0.07	0.07	0.07
Amplitude	1.0	0.9	0.7	0.44	0.28	0.22	0.14

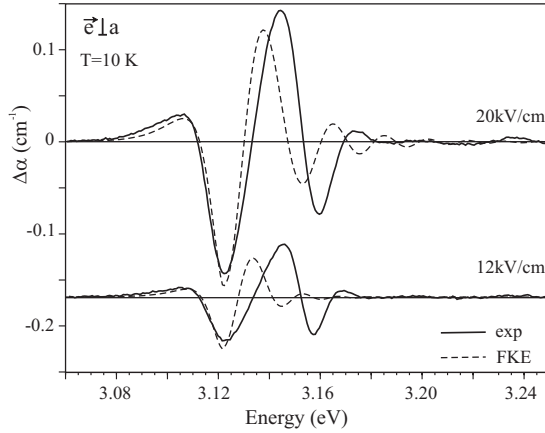


FIG. 13. Electroabsorption spectra at moderate fields compared to spectra of the one-dimensional Franz-Keldysh effect (dashed lines).

electron-hole pair gets resonant to vibrational modes. Vibrational excitons appear in absorption spectra 100 meV above the exciton. They limit unperturbed Franz-Keldysh oscillations to a range of 100 meV which in a field of 30 kV/cm corresponds to coherent motion over more than 300 Å.

The calculated spectra use scaling energies  $\hbar\theta$  of 22.93, 19.68, and 16.24 meV, respectively, which correspond to a reduced mass  $\mu=0.08m_0$ . A mass of  $0.09m_0$  reproduces the peak positions at 50 kV/cm too while a smaller mass of  $0.07m_0$  improves the fit to the spectrum at 30 kV/cm. Such small reduced mass is consistent with field broadening of the EA spectrum which requires fields that exceed the perturbation regime,  $\hbar\theta > \Gamma$ . It is emphasized that the mass of  $0.05m_0$  derived from field-broadening of the EA spectra of DCH and 3BCMU is far too small to match the numerous Franz-Keldysh oscillations observed for poly-3NPh2.

### 3. Spectra at small electric fields

Since the Franz-Keldysh effect neglects all correlation effects its excellent agreement with the data indicates that fields exceeding 30 kV/cm diminish other perturbations of free-electron states. Coulomb coupling of electron and hole should show up in spectra at smaller fields as deviation from the spectral line shape of the Franz-Keldysh effect. Such deviations appear at moderate fields as presented in Fig. 13. The leading positive and negative peaks are still reproduced with a slight increase in the gap to 3.122 eV but not the peaks at higher energy. The calculations predict narrower spectra and above 3.14 eV smaller peaks than actually observed. Spectra at 12 kV/cm show these distortion quite clearly by an experimental spectrum that extends beyond the Franz-Keldysh oscillations of a gap at 3.122 eV. It should be mentioned that by shifting the second positive peak of the Franz-Keldysh effect to the experimental peak at 3.146 eV the position of the subsequent peaks is reproduced again which points to a larger gap at smaller field.

Spectra at very small fields, 8 and 4 kV/cm are displayed in Fig. 14. Franz-Keldysh oscillations of a gap at 3.122 eV vanish 30 meV above the gap where the data still show a strong positive peak at 3.146 eV. Subsequent peaks shift with

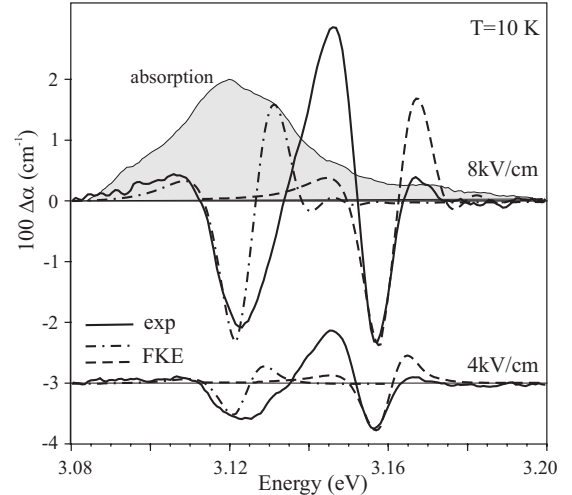


FIG. 14. EA spectra at small fields compared with the Franz-Keldysh effect of gaps at 3.122 eV (dashed-dotted) and 3.158 eV (dashed).  $\Gamma=10$  meV. The shaded area shows the weak absorption peak at 3.12 eV reduced by a factor of 500 to fit into the scale of the ordinate.

the field strength, and as shown by the dashed lines, their position is reproduced by the Franz-Keldysh effect if the gap is increased to 3.158 eV. The resulting line shape, a leading strong positive peak followed by a negative peak of similar size and weaker oscillations at higher energy is that observed for blue chains of 3BCMU and DCH. The most likely explanation for the large positive peak below the gap is a dipole-forbidden exciton which gains oscillator strength by mixing with the free-electron continuum<sup>34</sup> and such shallow dipole forbidden state has been predicted by theory.<sup>35,36</sup> We conjecture that the band gap of poly-3NPh2 lies at 3.158 eV and is defined by the Franz-Keldysh effect at small fields. This assignment yields a satisfactory description of the spectrum above 3.15 eV.

This assignment requires another interpretation of the high-field spectra with the gap at 3.120 eV and of the absorption peak Xc. Coulomb interaction of electron and hole generates not only bound states but transfers oscillator strength of electron-hole pairs from the continuum to bound states.<sup>37</sup> It is likely that the strong coupling of electron and hole confined to a narrow quantum wire removes the singularity of the density of states at the gap which explains the absence of a corresponding absorption peak in conjugated polymers. We therefore attribute the absorption peak Xc to a dipole-allowed exciton at 3.120 eV which has about 5% of the strength of the fundamental exciton. Field-induced coupling of this exciton to a forbidden state near 3.146 eV and to the free-carrier continuum passes from the low-field regime of the quadratic Stark effect to a high-field regime where bound excitons are ionized and become part of the continuum.<sup>38-41</sup> The gradual transition from the Stark effect of a bound exciton to field ionization has been observed in cubic semiconductors.<sup>28</sup> The excitonic signal changes its lineshape to that of a field-broadened state which joins the continuum when the field-induced potential across the exciton radius is about half the binding energy. With further increasing fields the exciton state is no longer resolved but marks the first

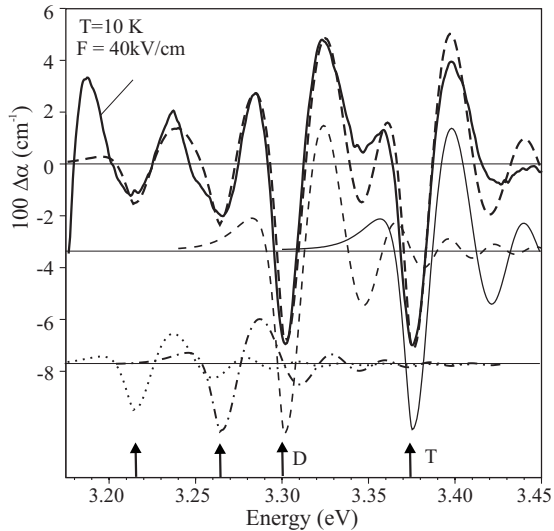


FIG. 15. EA spectrum at vibronic gaps (full curve) compared with the sum of four vibronic replica of the Franz-Keldysh effect (dashed curve). Their individual contribution is shown below with the corresponding energy gaps marked by arrows.

negative peak of Franz-Keldysh oscillations. Distortion of the Franz-Keldysh effect is evident in the spectra at 20 kV/cm and attributed to decoupling the exciton at 3.120 eV from that at 3.146 eV which is still part of the continuum. Taking 20 kV/cm as critical field for strong mixing estimates the exciton radius to 60 Å.

The exciton Xc at 3.120 eV responds to very small field by the quadratic Stark effect. A field of 4 kV/cm shifts an exciton of 60 Å radius and 38 meV binding energy by 0.15 meV and transfers almost 1% of its oscillator strength. Corresponding shift and decreasing size of the absorption peak predict an EA spectrum with an asymmetric negative peak of 0.15 cm<sup>-1</sup> amplitude. The negative EA peak at 3.122 eV is smaller by a factor 3 which points to a smaller radius of about 40 Å. The  $\Delta\alpha$  spectrum is also narrower and weak fine structure around 3.13 eV suggests some splitting of exciton Xc, similar as the fundamental exciton at 2.4 eV. We conjecture that the EA spectrum at small field resolves a weak dipole allowed exciton at 3.120 eV of large radius (40–60 Å) and a forbidden exciton at 3.146 eV which distorts the lineshape of the Franz-Keldysh effect of the gap at 3.158 eV.

#### 4. Vibronic replica of the Franz-Keldysh effect

EA spectra above the gap are described by the superposition of the Franz-Keldysh effect of four vibronic gaps with the same mass and broadening as for the gap itself (Fig. 15). The strongest replica D and T generate their own Franz-Keldysh oscillations with gaps at 3.301 and 3.374 eV, respectively, and the vibronic energies of 181 and 254 meV, counted from the high-field gap of 3.120 eV, are in accordance with the energies derived from the exciton spectra. The negative peaks at 3.264 and 3.215 eV correspond to vibrational energies of 144 and 95 meV and represent the joint response of two groups of modes which are better resolved in the exciton spectra. The vibronic spectra overlap

with the last member of Franz-Keldysh oscillation from the gap at 3.20 eV. Additional oscillations at higher energy are suppressed by resonant scattering of an electron-hole pair by vibrational modes and are substituted by oscillations of a correspondingly shifted gap. Similar to vibronic excitons coupling of free electron-hole pairs and vibrational modes provides resonances for the interband polarization which generates vibronic replicas of the energy gap. Field-broadening of these replicas is observed only if they are sufficiently separated as in case of double and triple bonds. It is pointed out that the EA spectrum presented in Fig. 4 resolves replica at 3.559 and 3.641 eV which are attributed to combination modes D+T and 2T, respectively, and appear also in the excitonic spectrum.

The vibrational replicas D and T at 12 kV/cm have the lineshape of the Franz-Keldysh effect in the low-field regime (Fig. 8), two positive peaks framing a strong negative peak at the gap. The reference energy for the vibronic energies is still the high-field gap at 3.12 eV, the energy of an ionized exciton state as part of the free-electron continuum. Since the signal decreases rapidly at smaller fields it was not possible to observe the separation of weakly bound excitons from the gap in the vibronic spectra.

#### V. SUMMARY AND CONCLUSIONS

Electroabsorption spectra of  $\pi$ -conjugated chains of 3NPh2 reveal significant changes of the electronic structure if the polymer repeat unit consists of two nonequivalent C<sub>4</sub> units. The optical gap, defined by a strong exciton has increased to 2.399 eV, larger than in any other polydiacetylene. Even larger is the increase in the band gap to 3.158 eV and of the exciton binding energy to 759 meV, compared to 485 meV in DCH (Ref. 9) and 560 meV in blue chains of 3BCMU (Ref. 10) and of THD (Ref. 19) Consistent with the increased binding energy is the decrease in the exciton radius to 6 Å. The exciton is still of the Wannier type since it extends over five conjugated bonds. These changes are attributed to reduced coupling of the C<sub>4</sub> units due to their twisted molecular planes. The twisting angle should be larger than the value of  $\pm 7.5^\circ$  reported for THD (Ref. 18) since in that material the exciton shows only a moderate increase in the transition energy to 2.171 eV and no significant change in the binding energy.

Poorer overlap of the neighboring C<sub>4</sub> units reduces the corresponding charge transfer integral and the width of the free-carrier bands. Since the  $\pi$  bonds have not changed, the splitting of  $\pi$  and  $\pi^*$  states which broaden to the valence and conduction bands is the same but a reduction in the band width increases the fundamental gap at the centre of the Brillouin zone. Doubling the polymer repeat unit reduces the size of the Brillouin zone while the number of subbands increases as band states are folded back into the reduced Brillouin zone. New gaps appear on the edge of this Brillouin zone which decrease the curvature of conduction and valence bands at the centre of the Brillouin zone. We propose that this effect and the smaller band width due to a reduced transfer integral between rotated C<sub>4</sub> units increases the reduced effective mass at the gap of poly-3NPh2 compared to the mass in blue chains.

The large exciton binding energy is consistent with its increased reduced mass and moves the band gap well beyond the range of vibrational excitons which enabled a detailed study of free-electron states in a one-dimensional system. The excellent agreement of the EA spectra at fields exceeding 30 kV/cm with the lineshape of the Franz-Keldysh effect points to strongly reduced electron correlation effects. Resonant coupling to molecular vibrations limits the range of unperturbed Franz-Keldysh oscillations to about 100 meV which yields a coherence range of band states larger than 300 Å, equivalent to 120 conjugated bonds.

Matching the Franz-Keldysh effect to the experimental spectra yields the parameters in Table III. The scaling energy  $\hbar\theta$  determines the spectral line shape if it exceeds the broadening parameter  $\Gamma=10$  meV and yields the reduced mass  $\mu=0.08m_0$ . The small mass supports wide energy bands predicted by band-structure calculations.<sup>20,21,35,42,43</sup> Assuming the same electron and hole mass yields a free-carrier mass of  $0.16m_0$  and an exciton mass of  $M=0.32m_0$  for the centre of mass motion which is in accordance to the value  $0.3m_0$  estimated from the radiative lifetime of excitons in red chains of 3BCMU.<sup>11,12</sup> The amplitude of the EA spectra which is defined by the interband matrix elements has been fitted to the leading peaks of Franz-Keldysh oscillations and is normalized to the value at the highest field. The amplitude nevertheless decreases with decreasing field since the imaginary part  $\eta=\Gamma/\hbar\theta$  of the renormalized energy of electron-hole pairs increases. Their Coulomb coupling leads to weakly

bound excitons states which are ionized in high fields and become part of the free carrier continuum. The energy gap at high fields which denotes the threshold to that continuum therefore occurs at 3.120 eV, the energy of an ionized exciton state with 38 meV binding energy. A small but distinct absorption peak indicates that this exciton is dipole allowed. It is emphasized that such weakly bound dipole allowed exciton has not been observed in other polydiacetylenes. The exciton decouples from band states in low fields and the corresponding spectra yields a gap at 3.158 eV with Franz-Keldysh oscillations which match a slightly smaller mass of  $0.07m_0$ . These spectra show a strong positive peak at 3.146 eV which is attributed to the field-induced gain of oscillator strength of a dipole forbidden exciton of 12 meV binding energy. This state provides a resonance in the free-electron continuum which modifies the shape of the Franz-Keldysh effect. This dipole forbidden exciton seems common to polydiacetylene chains since their EA spectra at the gap have the same lineshape as observed for poly-3NPh2 at small fields.

#### ACKNOWLEDGMENTS

Partial financial support of this work by the Agence Nationale pour la Recherche, France is acknowledged (Grant No. ANR-06-NANO-013). We are indebted to Charlotte Bourgeois from INSP for performing some of the  $\gamma$ -ray irradiations.

- 
- <sup>1</sup>G. Wegner, Z. Naturforsch. B **24**, 824 (1969).  
<sup>2</sup>R. H. Baughman, J. Polym. Sci., Part B: Polym. Phys. **12**, 1511 (1974).  
<sup>3</sup>G. Wegner, Pure Appl. Chem. **49**, 443 (1977).  
<sup>4</sup>R. H. Baughman and K. C. Yee, J. Polym. Sci. Macromol. Rev. **13**, 219 (1978).  
<sup>5</sup>D. Bloor, in *Developments in Crystalline Polymers I*, edited by D. C. Bassett (Applied Science Publisher, London, 1982), Chap. 4, p. 151.  
<sup>6</sup>D. Bloor, Mol. Cryst. Liq. Cryst. **93**, 183 (1983).  
<sup>7</sup>V. Enkelmann, Adv. Polym. Sci. **63**, 91 (1984).  
<sup>8</sup>G. Weiser, Phys. Rev. B **45**, 14076 (1992).  
<sup>9</sup>L. Sebastian and G. Weiser, Phys. Rev. Lett. **46**, 1156 (1981).  
<sup>10</sup>A. Horvath, G. Weiser, C. Lapersonne-Meyer, M. Schott, and S. Spagnoli, Phys. Rev. B **53**, 13507 (1996).  
<sup>11</sup>F. Dubin, J. Berréhar, R. Grousson, T. Guillet, C. Lapersonne-Meyer, M. Schott, and V. Voliotis, Phys. Rev. B **66**, 113202 (2002).  
<sup>12</sup>R. Lécuyer, J. Berréhar, J. D. Ganière, C. Lapersonne-Meyer, P. Lavallard, and M. Schott, Phys. Rev. B **66**, 125205 (2002).  
<sup>13</sup>F. Dubin, J. Berréhar, R. Grousson, M. Schott, and V. Voliotis, Phys. Rev. B **73**, 121302(R) (2006).  
<sup>14</sup>F. Dubin, R. Melet, T. Barisien, R. Grousson, L. Legrand, M. Schott, and V. Voliotis, Nat. Phys. **2**, 32 (2006).  
<sup>15</sup>L. Legrand, A. Al Choueiry, J. Holcman, A. Enderlin, R. Melet, T. Barisien, V. Voliotis, R. Grousson, and M. Schott, Phys. Status Solidi B **245**, 2702 (2008).  
<sup>16</sup>G. Weiser and J. Berréhar, Phys. Rev. Lett. **99**, 196401 (2007).  
<sup>17</sup>G. Weiser, J. Berréhar, and M. Schott, Phys. Rev. B **76**, 205201 (2007).  
<sup>18</sup>V. Enkelmann and G. Schleier, Acta Crystallogr., Sect. B: Struct. Crystallogr. Cryst. Chem. **36**, 1954 (1980).  
<sup>19</sup>T. Barisien, L. Legrand, G. Weiser, J. Deschamps, M. Balog, B. Boury, S. G. Dutremez, and M. Schott, Chem. Phys. Lett. **444**, 309 (2007).  
<sup>20</sup>J.-S. Filhol, J. Deschamps, S. G. Dutremez, B. Boury, T. Barisien, L. Legrand, and M. Schott, J. Am. Chem. Soc. **131**, 6976 (2009).  
<sup>21</sup>J. Deschamps, M. Balog, B. Boury, M. Ben Yahia, J.-S. Filhol, A. van der Lee, A. Al Choueiry, T. Barisien, L. Legrand, M. Schott, and S. D. Dutremez, Chem.-Eur. J. (to be published).  
<sup>22</sup>A. Al Choueiry, T. Barisien, J. Holcman, L. Legrand, M. Schott, G. Weiser, M. Balog, J. Deschamps, S. G. Dutremez, J.-S. Filhol, preceding paper, Phys. Rev. B **81**, 125208 (2010).  
<sup>23</sup>M. Born and E. Wolf, *Principles of Optics* (Cambridge University Press, Cambridge, 1997).  
<sup>24</sup>M. Schott, S. Spagnoli, and G. Weiser, Chem. Phys. **333**, 246 (2007).  
<sup>25</sup>D. E. Aspnes, Phys. Rev. **147**, 554 (1966).  
<sup>26</sup>P. Handler, S. Jaspersen, and S. Koeppen, Phys. Rev. Lett. **23**, 1387 (1969).  
<sup>27</sup>C. Van Hoof, K. Deneffe, J. DeBeck, D. J. Arent, and G. Borgh, Appl. Phys. Lett. **54**, 608 (1989).  
<sup>28</sup>A. Jaeger and G. Weiser, Phys. Rev. B **58**, 10674 (1998).

- <sup>29</sup>D. E. Aspnes, Phys. Rev. **153**, 972 (1967).
- <sup>30</sup>D. E. Aspnes and N. Bottka, in *Semiconductors and Semimetals Vol. 9: Modulation Techniques*, edited by R. K. Willardson and A. C. Beer (Academic Press, New York, 1972), Chap. 6.
- <sup>31</sup>G. Weiser and A. Horvath, in *Primary Photoexcitations in Conjugated Polymers: Molecular versus Semiconductor Band Model*, edited by N. S. Sariciftci (World Scientific, Singapore, 1997), Chap. 12.
- <sup>32</sup>A. Jaeger, G. Weiser, P. Wiedemann, I. Gyuro, and E. Zielinski, J. Phys.: Condens. Matter **8**, 6779 (1996).
- <sup>33</sup>R. Abramovich and I. A. Stegun, *Handbook of Mathematical Functions*, Applied Mathematics Series 55 (National Bureau of Standards, Washington, DC, 1966), p. 446.
- <sup>34</sup>G. Weiser, A. Horvath and H. J. Kolbe, Proc. SPIE **3145**, 152 (1997).
- <sup>35</sup>S. Abe, J. Phys. Soc. Jpn. **58**, 62 (1989).
- <sup>36</sup>D. Guo, S. Mazumdar, S. N. Dixit, F. Kajzar, F. Jarka, Y. Kawabe, and N. Peyghambarian, Phys. Rev. B **48**, 1433 (1993).
- <sup>37</sup>R. J. Elliott, Phys. Rev. **108**, 1384 (1957).
- <sup>38</sup>H. I. Ralph, J. Phys. C **1**, 378 (1968).
- <sup>39</sup>J. D. Dow and D. Redfield, Phys. Rev. B **1**, 3358 (1970).
- <sup>40</sup>D. F. Blossey, Phys. Rev. B **2**, 3976 (1970).
- <sup>41</sup>D. F. Blossey, Phys. Rev. B **3**, 1382 (1971).
- <sup>42</sup>S. Suhai, Phys. Rev. B **29**, 4570 (1984).
- <sup>43</sup>S. Abe, M. Schreiber, W. P. Su, and J. Yu, Phys. Rev. B **45**, 9432 (1992).